# ENHANCEMENT OF THE RAMAN SCATTERING AND THE THIRD-HARMONIC GENERATION IN SILICON NANOWIRES

Authors:

L.A. Golovan, K.V. Bunkov, K.A. Gonchar, V.Yu. Timoshenko, L.A. Osminkina, D.V. Petrov, V.S. Marshov, V.A. Sivakov, M.N. Kulmas

Corresponding author:       L.A. Golovan

                    e-mail:      golovan@physics.msu.ru

# Enhancement of the Raman Scattering and the Third-Harmonic Generation in Silicon Nanowires

L.A. Golovan[1,2], K.V. Bunkov[1], K.A. Gonchar[1], V.Yu. Timoshenko[1], L.A. Osminkina[1], D.V. Petrov[3], V.S. Marshov[1], V.A. Sivakov[4], M.N. Kulmas[4]

[1] Physics Department, M.V. Lomonosov Moscow State University, Moscow, 199991, Russia
[2] NRC 'Kurchatov Institute', Moscow, 123182, Russia
[3] D.V. Skobeltsyn Nuclear Physics Institute, M.V. Lomonosov Moscow State University, Moscow, 199991, Russia
[4] Institut für Photonische Technologien, Jena, D-07745, Germany

## Abstract

We studied features of Raman scattering and the third-harmonic generation in silicon nanowire (SiNW) ensembles formed by means of chemical etching of crystalline silicon (c-Si) wafers with preliminary deposited silver nanoparticles in hydrofluoric acid. The c-Si wafers of different crystallographic orientations and doping levels were used, which results in variations of the formed nanostructure size and degree of order. For the excitation at 1064 nm the ratio of Raman scattering signals for SiNWs and those for initial c-Si wafer ranges from 2 to 5, whereas for shorter wavelengths the ratio increases for more ordered arrays of SiNWs of greater diameter and decreases for less ordered SiNW structures. The TH signals in SiNW ensembles demonstrate both fall and one- or two-orders-of-magnitude rise in comparison with c-Si depending on the structure of the SiNW ensemble. The obtained results are explained by the effect of partial light localization in SiNW ensembles.

## Introduction

Silicon photonics, successfully combining achievements of the most developed semiconductor and optics technologies is one of the most prospective modern trends in optical and electronic engineering (see e.g. [1]). In particular, arrays of silicon one-dimensional nanostructures (nanowires) attract more and more interest of researchers due to large potential of their applications in photonics, electronics, and sensing [2-10]. The arrays consist of crystalline silicon (c-Si) wires of 20-200 nm in diameter and of 1-200 μm in length. These structures have been known since mid-60's, when they were formed by vapour-liquid-solid (VLS) technique [11] with the help of gold nanoparticles forming low-temperature eutectic with silicon.

For all mentioned applications crystallinity of the silicon nanowires (SiNWs), their geometry, surface oxide, impurity concentrations are of great importance. For SiNWs formed by VLS technique special attention should be paid to gold contamination of silicon, which affects optoelectronic properties of SiNWs [12].

Novel technique of metal-assisted chemical etching (MACE) [13-15] is free from the mentioned drawbacks. It employs a two-stage chemical process: at the first stage silver nanoprarticles are chemically deposited at the c-Si surface, whereas at the second stage they act as catalysts controlling the macropore etching in c-Si. If it is necessary, the silver nanoparticles can be removed by rinsing in nitric acid ($HNO_3$). The SiNWs formed by MACE are ordered straight or zig-zag SiNWs [13], which demonstrate enhancement of spontaneous Raman scattering, coherent anti-Stokes Raman scattering and silicon interband photoluminescence (PL) efficiency [16,17] in comparison with c-Si as well as visible PL caused by occurrence of Si nanocrystals due to stain etching process at the SiNW walls [14]. These features of SiNWs together with their extremely low (about 1%) total reflection [18,19] in visible range make this material very promising for various applications in photonics, photovoltaics and sensing.

In this paper, we discuss interrelation between structural and optical properties of SiNWs and their influence on the efficiency of such processes as Raman scattering and the third-harmonic generation.

## Experimental

In the experiment, samples of SiNW ensembles obtained at different in doping and surface orientation surfaces of c-Si were used. The c-Si substrates were rinsed in 49% HF solution for 1 min to remove native oxide coverage. Then, Ag nanoparticles of different morphology were deposited on surfaces of the substrates by immersing them in aqueous solution of 0.02M of silver nitrate ($AgNO_3$) and 5M of HF in the volume ratio of 1:1 for 30-60 sec. In the second step, the c-Si substrates covered with Ag nanoparticles were

immersed in a 50 ml of the solution containing 5M of HF and 30% $H_2O_2$ in the volume ratio 10:1 in a teflon vessel for time varied from 1 to 120 min. The duration of the second step determines the thickness of the SiNW layer [18]. Finally, the samples were rinsed several times in de-ionized water and dried at room temperature. Then, SiNW arrays were rinsed in a concentrated (65%) $HNO_3$ for 15 min to remove residual Ag nanoparticles from the SiNWs. Information about the different types of employed samples is collected in Table 1 and their SEM images are shown in Fig. 1. To study influence of the sample thickness on the efficiency of the Raman scattering we also prepared a set of C-types samples of different thickness varied from 2 to 70 nm.

Table 1: Nanowire ensembles and their typical sizes

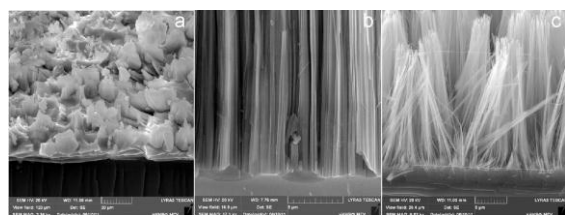| # | Doping | Specific resistance, Ohm·cm | Surface orientation | Nanowire diametre, nm |
|---|--------|------------------------------|---------------------|------------------------|
| A | As (*n*) | 0.001-0.005 | (111) | - |
| B | B (*p*) | 0.7-1.5 | (100) | 50-200 |
| C | B (*p*) | 1-20 | (111) | 100-350 |



Fig.1 SEM images of cuts of SiNW layers in samples A (a), B (b), and C (c).

Experiments on Raman scattering were carried out with the help of micro-Raman spectrometer Horiba Jobin Yvon HR 800 with excitation at wavelengths of 488 and 633 nm and Fourier-transform spectrometer Bruker IFS 66 V/S equipped with Raman scattering unit FRA-106 FT (excitation at 1064 nm). Maximal intensity of the laser radiation does not exceed 5 W/cm$^2$ (for 1064 nm), 500 W/cm$^2$ (for 633 nm), and 1200 W/cm$^2$ (for 488 nm). Under the mentioned intensities no significant heating of the samples took place, which was controlled by ratio of Stokes/anti-Stokes signals and linear dependence of the Raman signal on excitation intensity. The third-harmonic (TH) generation was pumped by quasi-cw Cr:forsterite laser (Avesta) (1250 nm, 80 fs, 150 mW, 80 MHz). The laser radiation was focused on the sample at the angle of incidence of 45° by a short-focus lens (F.L.=7.5 mm), whereas TH signal was collected by a lens with F.L.=15 mm and N.A.=0.6. Filters KG3 and FS were employed to select TH signal (417 nm). The photon-counting tube H7421 (Hamamatsu) was employed for the TH detection. Simultaneous rotation of the half-wave plate before the sample and an analyser after the sample allowed

us to obtain orientation dependences of the TH signal.

## Results

Fig. 2 presents typical PL and Raman scattering spectra of the SiNWs under the excitation at 1064 nm. One can see a broad band of interband transition in c-Si and a relatively sharp Raman peak at 520 cm$^{-1}$ corresponding to phonon frequency in c-Si. The PL and Raman signals of SiNWs several times exceed corresponding signals from c-Si substrate. Moreover, orientation dependence of the Raman signal evidences that for SiNWs symmetry of the signal is lost (cf. four-fold symmetry for c-Si and isotropic orientation dependence for SiNWs grown on it) (Fig. 3).
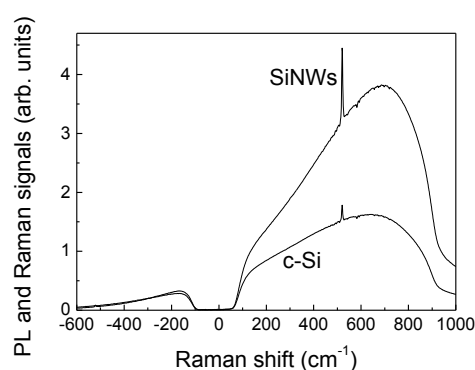


Fig.2 PL and Raman spectra for the SiNWs (sample B) and corresponding c-Si substrate excited by radiation at 1064 nm. A dip at around 0 cm$^{-1}$ is attributed to the transmission properties of the employed notch filter.
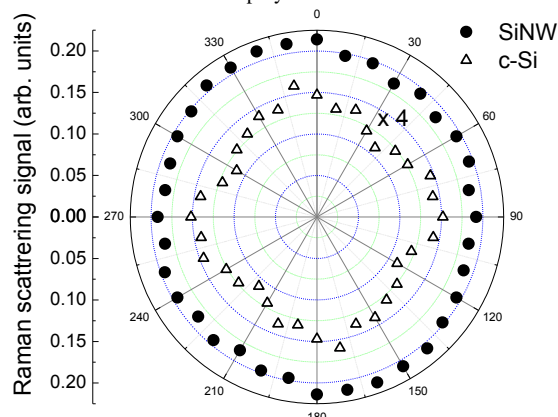


Fig. 3. Orientation dependence of SiNWs (sample C) and c-Si.

The obtained results are explained by the strong light scattering in SiNW resulting in the light trapping. That is why it would be very instructive to study the influence of the SiNW layer thickness and the excitation wavelength on the efficiency of Raman scattering.

The results of the former dependence are shown in Fig. 4. As one can see, even at thickness of 1.5 nm is enough to increase Raman (Stokes) signal twice in comparison with c-Si. Further increase of the thickness results in rise of the Raman signal. As evidences this experiment, even SiNW length of

1.5 μm is enough to trap the light and significantly increase the photon life time in silicon.

Comparison of the Raman-scattering efficiency for three different samples of SiNWs for various wavelengths was carried out (Fig. 4). Since Raman-scattering efficiency depends on free-carrier concentration, which differs for the different samples, we should take ratio of Raman signal for SiNW $I_{SiNW}$ and corresponding crystal substrate $I_{wafer}$ (Fig. 5).
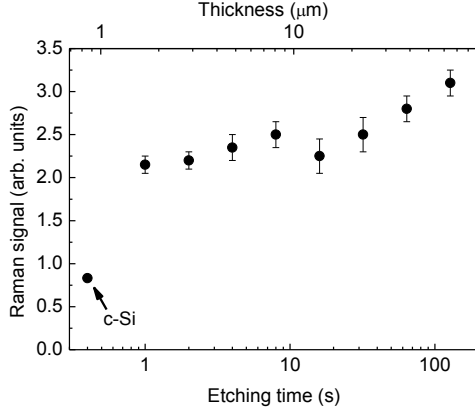


Fig. 4. The dependence of the Raman signal on the etching time and thickness of the SiNW sample (C-type samples).
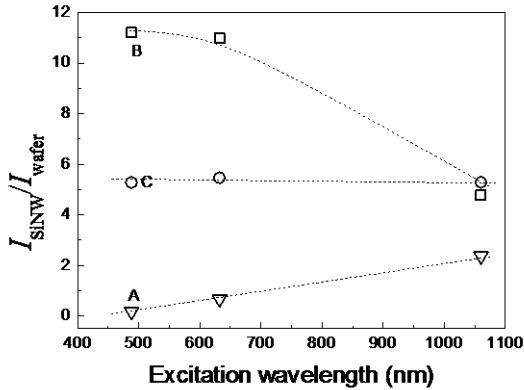


Fig. 5. Ratio $I_{SiNW}$ / $I_{wafer}$ vs. excitation wavelength for the samples A, B, and C.

For sample B $I_{SiNW}/I_{wafer}$ increases with the decrease of excitation wavelength, for sample C it is almost constant, whereas for sample A it falls.

The third-harmonic (TH) generation efficiency differs for the different samples (Fig. 6). Similar to the Raman scattering, the TH signal is minimal for the sample A and does not exceed one for c-Si, although it possesses another orientation dependences than c-Si (Figs. 6a, 6b). However, samples B and C demonstrate TH signal that exceed one for c-Si substrate one order of magnitude. Besides, orientation dependences for B and C samples are totally different from the dependences for their substrates. It is worth noting that for SiNWs when polarization of the TH is perpendicular to the fundamental radiation polarization TH signal is comparable to the TH for

parallel polarizations, although for c-Si TH signal for crossed polarizers is an order of amplitude weaker than for parallel ones. Both mentioned effects are certainly caused by the light scattering in SiNW ensembles.
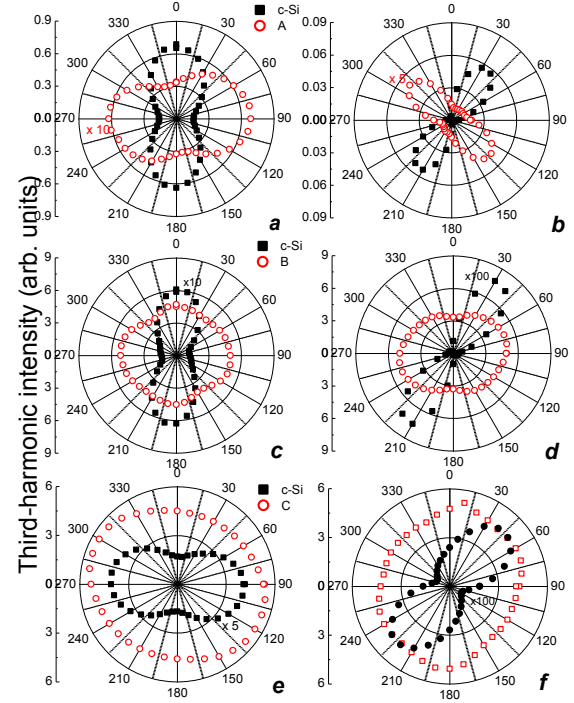


Fig. 6. Orientation dependences of TH for samples A (a, b), B (c, d), and C (e, f) for parallel (a, c, e) and perpendicular (b, d, f) polarizations of the TH and fundamental radiation. Angle of 0° corresponds to *p*-polarization of the fundamental radiation.

## Discussions

The reason of differences in Raman scattering and TH generation efficiencies for different samples is in their geometry, which affect the efficiency of the light localization and, hence, Raman and TH signals.

Discussing the variation of the Raman scattering efficiency with variations of the excitation wavelength we shall keep in mind interplay of two important factors: the light scattering and the light absorption. Both increases with the wavelength decrease. However, their actions are opposite: rise of the scattering efficiency results in increase of the photon lifetime in the medium, whereas the absorption reduces it.

All samples demonstrate $I_{SiNW}/ I_{wafer} >1$ for excitation wavelength of 1064 nm, which is characterized by low absorption. However, for the sample A possessing less ordered SiNWs effect of the light absorption is stronger than effect of the light scattering; as a results no light localization takes place. In contrast, more ordered SiNWs in the sample B does result in rather effective light localization, which is manifested in the rise of the Raman scattering efficiency. At last, the

sample C is in intermediate position, since its less ordered SiNWs (see Fig. 1) allow very moderate light localization, which is enough to compensate for absorptions [20].

The effects detected in experiments on TH generation in SiNWs have the similar reasons. Indeed, the rise of nonlinear-optical response in inhomogeneous Si-based media is well known (e.g. TH signal for mesioporous Si is more than oreder of amplitude more effective than c-Si [21]). Again, the TH enhancement is caused by the light localization effects, whereas the absorption at TH wavelength reduces efficiency of this process. Thus, the obtained TH generation results are in a good agreement with the results of Raman scattering experiments: sample A possessing badly ordered SiNWs demonstrates a fall of TH signal in comparison with c-Si since the light localization is not enough to overcame the light losses, whereas better-ordered samples B and C demonstrate an order or two-orders of magnitude more TH signal than c-Si.

Thus, in the carried out experiments we demonstrated both fall and one- or two-orders-of-magnitude rise of Raman and TH signals in SiNWs in comparison with c-Si depending on the structure of the SiNW ensemble. The obtained results as well as orientation dependences for Raman and TH signals and the dependence of the Raman signal on the SiNW layer thickness are manifistations of the partial light localization in SiNW ensembles.

## References

[1] D.J. Lockwood and L. Pavesi (eds.) (2011), Silicon Photonics II. Components and Integration, Topics in Applied Physics, 119 (Springer, Berlin – Heidelberg)

[2] P. Yang, R. Yan, and M. Fardy (2010), Semiconductor Nanowire: What's Next? Nano Lett., 10, 1529.

[3] J. Hu, M. Ouyang, P. Yang, and C.M. Lieber (1999), Controlled Growth and Electrical Properties of Heterojunctions of Carbon Nanotubes and Silicon Nanowires. Nature, 399, 48.

[4] H. Föll, H. Hartz, E. Ossei-Wusu, J. Carstensen, and O. Riemenschneider (2010), Si nanowire arrays as anodes in Li ion batteries. Phys. Status Solidi RRL, 4, 4.

[5] G. Bronstrup, N. Jahr, C. Leiterer, A. Csaki, W. Fritzsche, and S. Christiansen (2010), Optical Properties of Individual Silicon Nanowires for Photonic Devices. ACS Nano, 4, 7113.

[6] M.D. Kelzenberg, D.B. Turner-Evans, B.M. Kayes, M.A. Filler, M.C. Putnam, N.S. Lewis, and H.A. Atwater (2008), Photovoltaic Measurements in Single-Nanowire Silicon Solar Cells. Nano Lett., 8, 710.

[7] V. Sivakov, G. Andrä, A. Gawlik, A. Berger, J. Plentz, F. Falk, and S. H. Christiansen (2009), Silicon Nanowire-Based Solar Cells on Glass: Synthesis, Optical Properties, and Cell Parameters. Nano Lett., 9, 1549.

[8] Y. Cui, Q. Wei, H. Park, and C.M. Lieber (2001), Nanowire Nanosensors for Highly Sensitive and Selective Detection of Biological and Chemical Species. Science, 293, 1289.

[9] X. Wang, and C.S. Ozkan (2008), Multisegment Nanowire Sensors for the Detection of DNA Molecules. Nano Lett., 8, 398.

[10] V. Sivakov, S. Christiansen (2012), Novel Discovery of Silicon, J. of Nanoelectronics and Optoelectronics, 7, 583-590.

[11] R. S. Wagner, and W. C. Ellis (1964), Vapor-Liquid-Solid Mechanism of Single Crystal Growth. Appl. Phys. Lett., 4, 89.

[12] A. Bailly, O. Renault, N. Barrett, L.F.Zagonel, P. Gentile, N. Pauc, F. Dhalluin, T.Baron, A. Chabli, J.C. Cezar, N.B. Brookes (2008), Direct Quantification of Gold along a Single Silicon Nanowire. Nano Lett., **8**, 3709-3714.

[13]V.A. Sivakov, G. Bronstrup, B. Pecz, A. Berger, G.Z. Radnoczi, M. Krause, S.H. Christiansen (2010), Realization of Vertical and Zigzag Single Crystalline Silicon Nanowire Architectures. J. Phys. Chem. C **114**, 3798-3803.

[14] V. A. Sivakov, F. Voigt, A. Berger, G. Bauer, and S. H. Christiansen (2010), Roughness of Silicon Nanowire Sidewalls and Room Temperature Photoluminescence. Phys. Rev. B., 82, 125446.

[15] Z. Huang, N. Geyer, P. Werner, J. de Boor, and U. Gösele (2011), Metal-Assisted Chemical Etching of Silicon: A Review. Adv. Mater., 23, 285.

[16] V.Yu. Timoshenko, K.A. Gonchar, L.A. Golovan, A.I. Efimova, V.A. Sivakov, A. Dellith, and S.H. Christiansen (2011), Photoluminescence and Raman Scattering in Arrays of Silicon Nanowires. Journal of Nanoelectronics and Optoelectronics. 6, 519-525.

[17] L.A. Golovan, K.A. Gonchar, V.Yu. Timoshenko, G.I. Petrov, V.V. Yakovlev (2012), Coherent anti-Stokes Raman scattering in silicon nanowire ensembles. Laser Phys. Lett., 9, 145-150.

[18] K.A. Gonchar, L.A. Osminkina, R.A. Galkin, V.S.Marshov, D.V. Petrov, V.V. Solovyev, A.A. Kudryavtsev, V.A. Sivakov, V.Yu. Timoshenko (2012) Structure and optical properties of silicon nanowire arrays formed by metal-assisted chemical etching. J. of Nanoelectronics and Optoelectronics, 7, 602-606.

[19] L.A. Osminkina, K.A. Gonchar, V.S. Marshov, K.V. Bunkov, D.V. Petrov, L.A. Golovan, F. Talkenberg, V.A. Sivakov, V.Yu. Timoshenko (2012), Optical properties of silicon nanowire arrays formed by metal-assisted chemical etching: evidences for light localization effect, Nanoscale Research Lett., 7, 524.

[20] K.V. Bunkov, L.A. Golovan, K.A. Gonchar, V. Yu. Timoshenko, P.K. Kashkarov, M. Kulmas, V. Sivakov (2013), Dependence of Raman scattering efficiency in silicon nanowire arrays on excitation wavelength. Semiconductors, 47, no.3 (in press).

[21] L.A. Golovan, L.P. Kuznetsova, A.B. Fedotov, S.O. Konorov, D.A. Sidorov-Biryukov, V.Yu. Timoshenko, A.M. Zheltikov, P.K. Kashkarov (2003), Nanocrystal-size-sensitive third-harmonic generation in nanostructured silicon. Appl. Phys. B, 76, 429-433.